SSRG International Journal of Electronics and Communication Engineering Volume 12 Issue 11, 123-132, November 2025
ISSN: 2348-8549/ https://doi.org/10.14445/23488549/IJECE-V12I11P110

Original Article

A Small Ultra-Wideband mm Wave Antenna for WBAN and Advanced Wireless Communication Systems

Bharat W. Patil[1], Ashwini S. Kunte[2]

[1,2]*Thadomal Shahani Engineering College, Bandra (West) Mumbai-50, Maharashtra, India.*

[1]*Corresponding Author : bharatpatilumit@gmail.com*

Received: 10 September 2025 Revised: 12 October 2025 Accepted: 11 November 2025 Published: 29 November 2025

Abstract *- This study introduces a miniature rectangular microstrip patch antenna that functions across a broad bandwidth, encompassing both Ultra-Wideband (UWB) and millimeter-wave (mmWave) frequency bands. It is specifically designed with the aim of convergence of UWB and mm wave technologies, which can be a key enabler for next-generation Wireless Body Area Network (WBAN) applications along with 5G IoT wearable systems. The proposed antenna design features a small dimension of 13.85 mm × 14.05 mm, fabricated on a 0.254 mm thick semiflexible PTFE-based Rogers RT/5880 substrate. It employs a Simple Microstrip Rectangular Patch with a partial ground and an integrated slot for achieving a wider bandwidth, ensuring seamless coverage across the key UWB and mm Wave frequency bands. The proposed antenna exhibits a peak gain of 3.49 dBi and a directivity in the typical range of 2-4, along with high radiation efficiency and stable radiation patterns across the entire operating range, which are suitable for wearable antennas used in short-range communication. The close accord between the simulated outcomes and actual measurements confirms the efficacy of the proposed design. Specific Absorption Rate (SAR) analysis is further validating its suitability for on-body deployment with the values of 0.438 W/Kg for 9.1 GHz and 0.482 W/kg for 24.2 GHz, which are well below the guidelines as per FCC regulations, IEEE C95.1, and ICNIRP limits (1.6 W/Kg for 1 gm). With its wideband operation, favorable gain, high efficiency, and safe electromagnetic profile, the proposed compact antenna serves as a comprehensive solution for next-generation UWB mm wave WBAN systems along with 5G wearable IoT systems.*

Keywords *- Wireless Body Area Network (WBAN), Ultra-Wideband (UWB), millimeter-wave (mm Wave), SAR, Microstrip antenna, Radiation efficiency, Gain, Directivity, Body-centric communication.*

1. Introduction

The recent advancements of Internet technologies along with profound transformations in the wireless personal wireless connectivity scenario highlight the evolving panorama of Body Centric Wireless Communications Systems (BCWC). These are often known as Wireless Body Area Networks (WBAN), consisting of sensors and actuators positioned in, on, and around the human body to facilitate real-time observation, management, and communication [1].

Moreover, the rapidly growing field of wearable electronics, along with WBANs, is making it an integral element of our modern-day lives due to the development of various sophisticated applications, like continuous monitoring of vital health parameters in emerging home health care systems and advancements in sports analytics, entertainment, and military operations.

In particular, innovations like smart textiles and motion sensing have enhanced the potential of WBANs in dynamic environments like defence and athletic performance monitoring [2].

The unrelenting miniaturization of sensor technologies, along with increasing demand for real-time, untethered data collection ability, requires highly efficient and robust wireless system solutions. This has resulted in increasing demand for compact, lightweight, simple, thin, versatile, and conformal antennas capable of operating over broad frequency ranges, supporting high data rates, and providing ultra-reliable connectivity. Consequently, the antennas designed for modern-day personal wireless communication systems must achieve a careful balance among performance, mechanical flexibility, biocompatibility, user comfort, safety (SAR compliance), and ease of fabrication [3].

Antennas serve as the terminal component in all wireless communication systems, functioning as an interface between wireless devices and the surrounding medium. These are responsible for system performance and overall communication link quality, as well as the size of the entire system. Conventional systems were bulkier due to the significant space occupied by the antennas, owing to their rigid structures and fixed form factors [1]. However, the relentless trend towards miniaturization in consumer electronics and wearable devices due to advancements in semiconductor technology, resulting in highly integrated systems, makes it essential for antennas also to adapt through advanced design and fabrication techniques. This extends beyond the antenna size reduction and imposes the challenge of maintaining or even enhancing crucial performance parameters such as gain, efficiency, and bandwidth [4, 5]. In addition to these fundamental requirements, their use in a wider array of platforms like flexible displays, smart textiles, biomedical implants, compact IoT sensors, and particularly wearable gadgets requires that they must adapt to the human body's contours and movements. These requirements directly fuelled the intensive research into novel antenna architectures, materials, and design methodologies that can meet these stringent demands of size, user comfort, and device durability without compromising RF performance in WBAN as well as future wireless communications systems [3].

Ultra-Wideband (UWB) technology is effective for short-range wireless communication because it has high temporal resolution, low power consumption, and is resistant to multipath fading effects. These characteristics make it possible to achieve fast data transfer, accurate positioning, and low-latency sensing in Wireless Body Area Networks [6]. At the same time, millimetre-Wave frequencies usually range from 24 GHz to 60 GHz, with new use cases starting from 6 GHz and going up, offering very wide bandwidths which allow for multi-gigabit per second (Gbps) data rates that are necessary for 5G/6G, real-time video streaming, Augmented Reality (AR), and high-throughput links on the human body [7]. Thus, the convergence of UWB and mmWave technologies can become a transformative enabler for future wearable and advanced wireless communications due to their capability to create wireless connections that are safe, low-interference, and very reliable, even in crowded areas when built into wearable platforms. Though using UWB and mm Wave in wearables is promising, it is yet challenging because of the antenna design problems related to size, impedance matching, and human safety (e.g., SAR) [7, 8].

Despite the significant advancements in wearable antenna technologies, developing a single, compact, and flexible antenna that can maintain efficient performance across both UWB and mmWave frequency ranges remains a major design challenge. Most reported antennas either achieve wideband performance within limited frequency spans or have multiband characteristics. Few researchers have investigated super-band antennas, but they exhibit larger dimensions. Furthermore, antennas designed for wearable applications must sustain mechanical deformation, proximity effects, and environmental variations such as humidity and bending without compromising performance parameters like bandwidth, gain, or SAR. This necessitates a careful balance between electromagnetic performance, mechanical flexibility, and biocompatibility, which remains challenging to achieve in most existing designs.

Recent studies on the wearable UWB and mmWave antennas explored various substrate materials along with different structural designs, but notable gaps still remain. For instance, textile-based UWB antennas mostly prefer denim or polyester substrates, which offer flexibility but lack in providing dielectric instability, moisture sensitivity, and narrow bandwidth, which makes them unsuitable for high-frequency mmWave applications [5]. Polymer substrates like PDMS, LCP, and Kapton demonstrate better high-frequency coverage, but they have higher loss tangents (for example, PDMS tan $\delta \approx 0.134$) and need to be thicker than 0.5 mm to stay structurally sound, which makes them less flexible and harder to make [8]. These combined mechanical, dielectric, and processing constraints highlight a research gap for developing a small, thin, and flexible antenna that can simultaneously operate across UWB and mmWave bands while maintaining low SAR, broad bandwidth, and ease of fabrication, making it suitable for wearable systems.

The novelty of the proposed work lies in its ability to accomplish wideband performance that covers both UWB and mmWave bands with a single, rectangular antenna made from 0.254 mm-thick Rogers RT/5880 substrate. Unlike conventional textile or polymer-based designs, the proposed antenna obtains 22.41 GHz bandwidth over an operating frequency span of 7 GHz to 30 GHz, covering both UWB and mmWave regions. The SAR of 0.438 W/kg in the UWB range and 0.482 W/kg in the mmWave confirms its wearable characteristics, as these are significantly below the FCC’s regulation of 1.6 W/kg for an averaging mass of 1 gram of tissue. Overall, the proposed work attempts to bridge the gap between performance, size, ease of fabrication, and flexibility, offering a practical solution for next-generation WBANs and compact mmWave wearable systems.

This paper is structured as follows: Section II discusses the literature review. Section III addresses the methodology, followed by antenna design. The results of both the simulations and experimental work are examined in Section IV. Lastly, Section V wraps up the paper with a recap of the key findings and potential future directions.

2. Literature Review

Several authors have investigated, designed, and evaluated Microstrip Patch Antennas using various techniques for the UWB or mm waves band and super band for IoT and Body Centric Communication Systems.

An ultra-wideband dense rectangular patch antenna for IoT applications was proposed by MD Firoze et al., where the authors have used a combination of a slotted patch and partial defected ground structure in the design. An FR-4 epoxy substrate, 0.8 mm thick with tan $\delta \approx 0.02$, was utilized as a non-conductive material in the proposed design, which provides an operational bandwidth of 19.9 GHz [9]. This antenna is limited to applications in the UWB band and frequencies below 23 GHz with a size of 30 mm × 20 mm × 0.8 mm.

A printed monopole half-elliptical-shaped patch antenna was designed and evaluated by Fitri Yuli Zulkifli et al. Normally, a semicircular shape is the preferred choice for impedance bandwidth widening, but in this work, the authors have used a half-elliptical radiator along with a partial ground plane having a triangular inset in their proposed design.

The design was carried out on Taconic TLY-5 substrate, which offers a wider bandwidth of around 23 GHz (0.5 GHz-23.5GHz) and hence can be used for applications of the UWB band and frequencies up to 23.5 GHz [10]. This antenna is bulky with dimensions of 200 mm × 200mm × 1.57 mm.

A compact tri-band MIMO antenna design was proposed and evaluated by Ayyaz Ali et al., featuring multiple C- and L-shaped structures with a small slot cut in the partial ground plane. This 2×2 MIMO configuration operates in sub-6, Ku, and mmWave bands, with overall dimensions of 30 mm × 30 mm, built on a 0.254 mm Rogers RT/5880 substrate. Although the antenna covers a wide range of frequency bands, its complex geometry increases design difficulty and fabrication cost [11].

A Novel Wearable Fractal antenna for wideband applications is designed and simulated by S S Bhatia et al, which uses polyester material of 1 mm thickness and a dielectric constant of 3.2. Although the Proposed antenna supports a wider bandwidth from 4.3 GHz to 30 GHz, it is limited by moisture absorption due to issues with the textile substrate and metallization cracking [12].

A Novel design based on commercially available Rogers RO3008 laminate with thick copper metallization of 28.5 mm supporting a measured bandwidth of 67 GHz (158 GHz simulated) is proposed and investigated by S. Dey et al. in [13]. It has a size of 60mm × 40mm × 1.52mm with an additional metallisation patch with a thickness of 28.5 mm, resulting in a large and rigid structure that limits its adaptability for conformal or wearable systems.

Waqas Ali et al. developed a quad-band wearable antenna covering the S band, WLAN, RFID frequency band, and X band using a semiflexible substrate, RT 5880, having dimensions 25 mm × 40 mm × 1.5 mm. This comb-shaped antenna structure is designed to achieve SAR within permissible limits of below the guidelines as per FCC regulations in the UWB band, but limits the applicability for mmWave systems [14].

Wanwisa T. et al proposed an octagonal-shaped textile monopole antenna using felt fabric with a permittivity of 1.4 and 1 mm thickness, with a bandwidth of 3.1-10.6 (UWB Band) and a size of 30 mm × 40 mm × 1 mm [15]. However, it is constrained by UWB operational range, as well as moisture absorption and metallization cracking issues attributed to the textile substrate.

M. Ali et al. proposed an electromagnetic band gap-backed thin flexible antenna with an operating frequency range of 24-24.5 GHz. This antenna features a geometrical shape of a Slotted Bow tie on Rogers RT 5880 substrate, measuring 16.19 mm × 16.19 mm × 0.254 mm [16]. However, the narrow operational bandwidth restricts its usability for broadband or multi-band body-centric systems.

M.S. Fouad et al. have proposed a two-arm fractal antenna for future wireless communication systems, offering a total bandwidth of 27 GHz and an operating span of 3 GHz-30 GHz. Additionally, a novel SWB balun was integrated to feed the antenna, ensuring stable performance across the band. This antenna bears a dimension of 40 × 21 mm; however, the planar rigidity and lack of mechanical flexibility reduced its suitability for wearable or conformal use [17].

A detailed review of the current literature shows important developments in the microstrip antenna design for Ultra-Wideband, millimeter-wave, multi-band, and wide-band frequency applications for Internet of Things (IoT) and Body Centric Wireless Communication domains. Various researchers have used different techniques, such as creating slots of different shapes and sizes in the radiating element, using fractal geometries, utilizing partial or defective ground surfaces, and modifying the substrate height or permittivity for enhancing impedance matching and bandwidth performance. The choice of substrate material remains a critical factor as it directly affects antenna size and its high-frequency performance. Materials such as FR-4 and textile fabrics are low-cost and flexible, but they exhibit high dielectric losses and moisture sensitivity, which limit their reliability in high-frequency wearable systems.

On the other hand, high-performance substrates like Rogers RT/5880 and TLY-5 demonstrate better electrical stability and lower loss at microwave and mmWave frequencies but have relatively limited mechanical flexibility. Despite the various reported developments, most existing antenna designs are either relatively bulky or bear complex geometries. In addition, these normally operate over limited frequency ranges and face trade-offs between flexibility, bandwidth, ease of fabrication, and safety for wearable applications. These limitations highlight the requirement of small, thin, semi-flexible antenna designs that effectively operate across both UWB and mmWave frequency ranges, maintaining low SAR, making them suitable for future wearable and body-centric wireless systems.

To overcome these limitations, the present work proposes a novel wearable rectangular microstrip patch antenna designed on Rogers RT/5880 substrate, operating over both UWB and mmWave bands. The following section describes the methodology adopted in antenna design, simulation, and performance evaluation to achieve wideband operation with optimized flexibility, efficiency, and SAR compliance.

3. Antenna Design Methodology

The proposed antenna is designed with a systematic, methodical process involving various steps, which are discussed below.

3.1. Antenna Characterization and Substrate Selection

Characterization of the proposed wearable antenna has been done carefully, considering various desirable factors and requirements of the wearable antenna for WBAN and the modern communication systems used for biomedical, wearable, handheld, and future compact IoT systems. The non-conducting substrate material for our proposed antenna is selected after comparing the related work done in recent years, along with the electrical characteristics in both frequency bands, as well as the desired mechanical characteristics for a wearable antenna. The Proposed antenna is designed with Rogers RT/5880, which is a PTFE-based semi-flexible substrate with excellent stable electric characteristics at UWB, mm wave, and 5G frequencies. It has a Dielectric Constant ($\varepsilon_r \approx 2.2$) with tan $\delta \approx 0.0009$ that works better electrically with ultra-thin laminates [12]. It offers various advantages like low electric loss, minimal moisture absorption, excellent chemical resistance, isotropic properties, and uniform electrical properties over a wide range of operational frequency in UWB and mm Waves bands. Apart from these, it also satisfies the requirements of wearable antenna requirements, like flexibility and relatively stable bending properties. The Design specifications based on characterization are listed below.

1) Impedance =50 ohms
2) Substrate: Rogers RT/Duriod 5880
3) Thickness: 0.254 mm
4) Permittivity: 2.2
5) Loss tangent: 0.0009
6) Features: Simple, Compact, Thin, Semi-Flexible, Wearable, UWB mm Wave Microstrip Patch Antenna.

3.2. Microstrip Patch Antenna Design

The following design equations are used to first determine the antenna's geometrical parameters for a rectangular patch.

$$Wp = \frac{c}{2f_0\sqrt{\frac{\varepsilon_r+1}{2}}} \tag{1}$$

Where *Wp* is the width of the rectangular patch.

$$\varepsilon_{reff} = \frac{\varepsilon_r+1}{2} + \frac{\varepsilon_r-1}{2}\left[1+12\frac{h}{W_p}\right]^{-1/2} \tag{2}$$

$$\frac{\triangle L}{H} = 0.412\frac{(\varepsilon_{reff}+0.3)(\frac{W}{h}+0.262)}{(\varepsilon_{reff}-0.258)(\frac{W}{h}+0.813)} \tag{3}$$

$$L_p = \frac{c}{2f_0\sqrt{\varepsilon_{reff}}} - 2\triangle L \tag{4}$$

Where *Lp* is the length of the rectangular patch.

Based on the above mathematical design equations, a standard rectangular patch antenna with an inset feed is designed (Step 1) and simulated with CST Microwave.

The proposed antenna design is conducted in four steps, with rigorous parametric analysis performed on a standard patch antenna featuring an inset feed and a full ground plane (Step 1). Techniques such as partial ground plane and Defected Ground Surface (DGS) are applied in a stepwise manner to obtain the desired response. Figure1 below shows the stepwise response of the Reflection Coefficient during the design process. Figure 2 below shows the Stepwise changes in the geometry of the antenna.

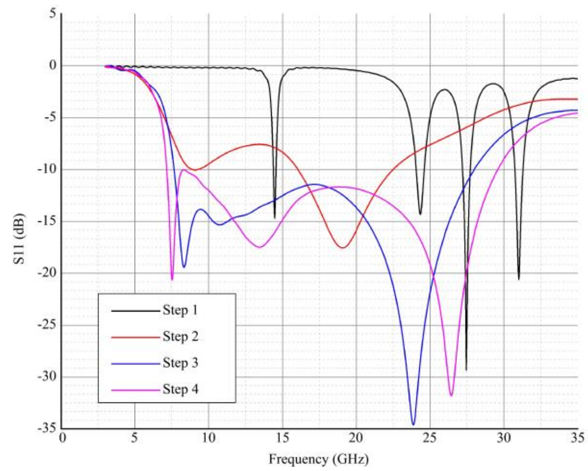

Fig. 1 Stepwise variation of the Reflection Coefficient

Reducing the dimensions of the ground plane results in reduced effective capacitance between the patch and ground plane, thereby decreasing the Q factor. This results in increased bandwidth ($\triangle f$) as these are inversely proportional as below.

$$\triangle f = \frac{f_0}{Q} \tag{5}$$

Where f_0= Resonant frequency

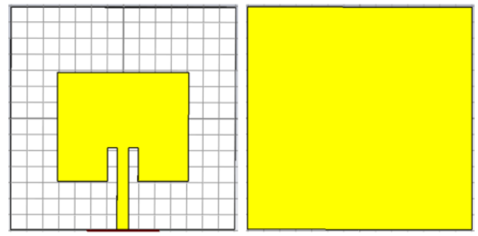

(a)

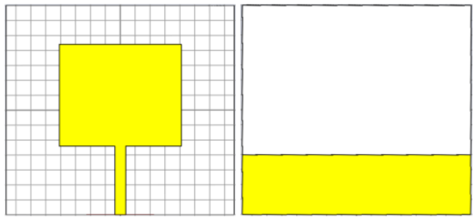

(b)

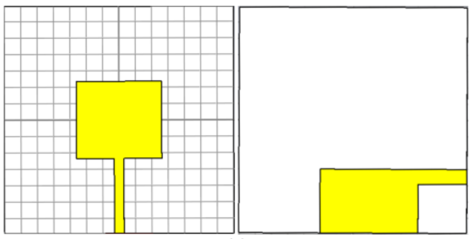

(c)

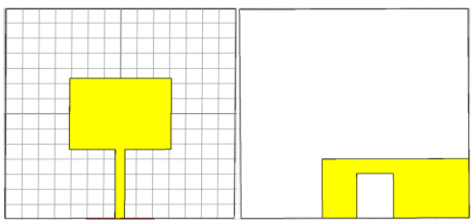

(d)

Fig. 2 Stepwise Design of Proposed Antenna: (a)Step 1, (b)Step 2, (c)Step 3, and (d)Step 4.

The inset feed is removed in step 2 to increase the mechanical strength of the proposed antenna, while also reducing design and fabrication complexity, thereby simplifying the overall design. Further enhancement in bandwidth was achieved by cutting a slot in the partial ground for the desired bandwidth. The physical parameters of the Proposed Antenna are provided in Table 1 and are shown in Figure 3 below.

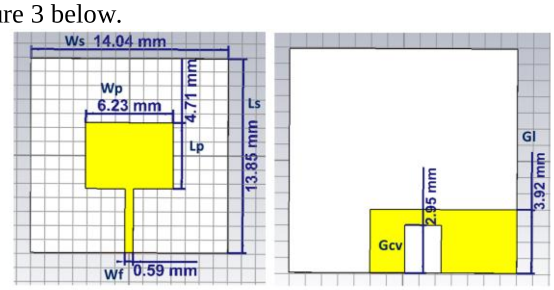

(a) (b)

Fig. 3 Proposed Antenna Structure: (a)Front, and (b)Back.

Table 1. Geometrical parameters of the proposed ultra-wideband -mm wave antenna.

Parameter	Value in mm	Parameter	Value in mm
Ws	14.04	***Gcv***	2.95
Ls	13.85	***Wf***	0.59
Wp	6.23	***Gl***	3.92
Lp	4.71	***Gw***	9.32

4. Results and Discussion

The proposed Ultra-Wide Band mm Wave Antenna is then simulated and optimised for obtaining various parameters of interest for evaluating its performance. Simulated results are discussed with plots of the respective responses below.

For evaluating the overall antenna performance, S_{11} (Reflection coefficient) and VSWR (Voltage Standing Wave Ratio) are the crucial parameters for impedance matching and power transfer efficiency. For antenna design, maintaining S_{11} below -10 dB and VSWR below 2 across the desired operating frequency range shows minimal power loss, improved radiation efficiency, and enhanced overall system performance. The simulated S11 response for the proposed antenna is shown below in Figure 4.

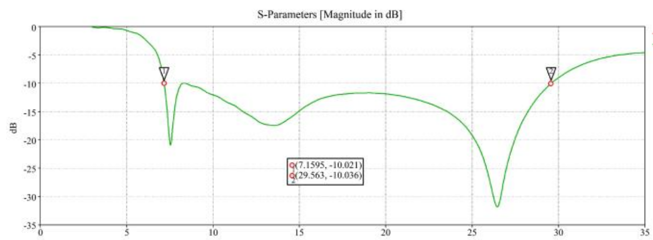

Fig. 4 S_{11} versus Frequency Response (Simulated) of the Proposed Antenna

The proposed antenna maintains a reflection coefficient consistently below the acceptable threshold of -10 dB, as shown in Figure 4, and VSWR below 2, as seen in Figure 5, across the extensive frequency span between 7.15 GHz and 29.56 GHz, covering both the UWB band as well as the mm wave band, showing the effective impedance matching over the mentioned frequency range. The total Impedance bandwidth occupied by the proposed antenna is almost 22.41GHz as per simulation results.

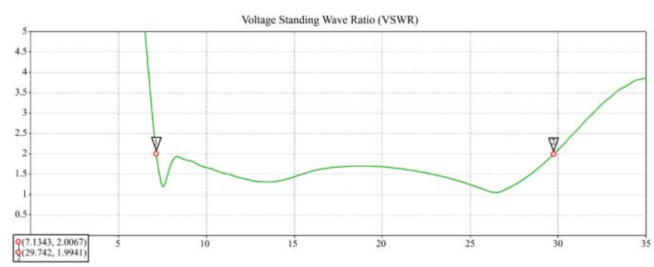

Fig. 5 Simulated VSWR Response of the Proposed Antenna

The effectiveness with which an antenna transmits or receives signals in a desired direction is measured by its antenna gain. This is an important parameter for wireless communication systems. The plot of Gain versus Frequency (Simulated) is shown below in Figure 6. This shows the gain increasing with frequency until a maximum gain of 3.37 dBi at 21 GHz, and then reducing to 2.12 dBi at 30 GHz over the operational bandwidth.

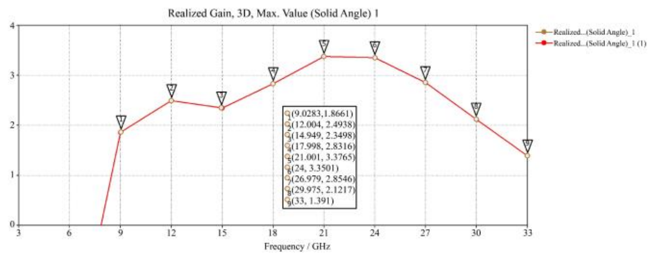

Fig. 6 Simulated Gain over Frequency plot of the Proposed antenna

Figure 7 below displays the simulated 3D far-field radiation patterns for various frequencies across the whole operational bandwidth. Results show that the proposed antenna shows a perfect omnidirectional pattern for a frequency of 9 GHz. However, with increasing frequencies with the emergence of side lobes due to excitation of higher order modes and Partial ground plane presence, the ideal radiation pattern is disrupted to some extent [10].

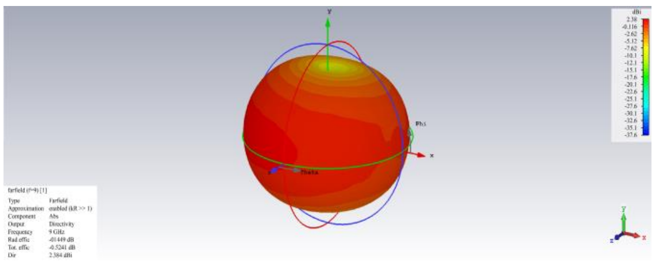

(a)

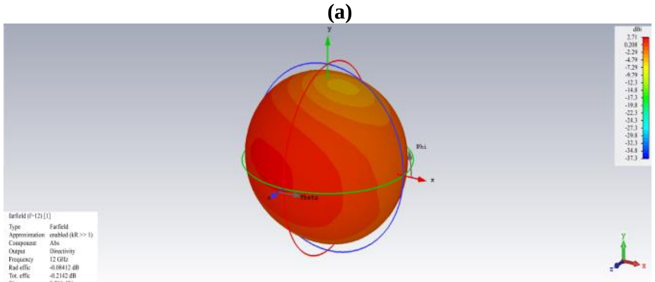

(b)

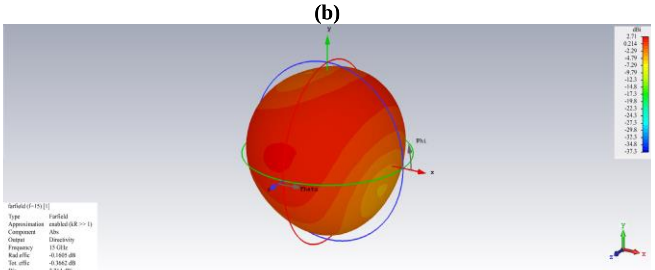

(c)

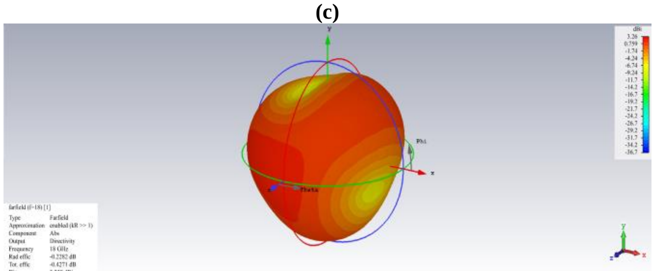

(d)

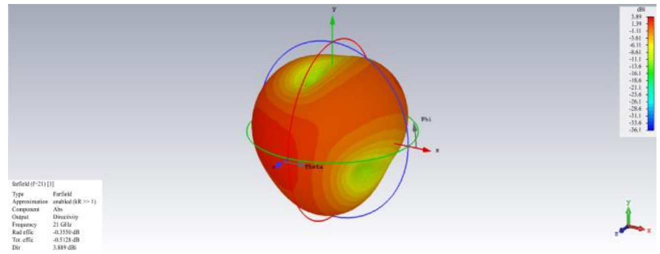

(e)

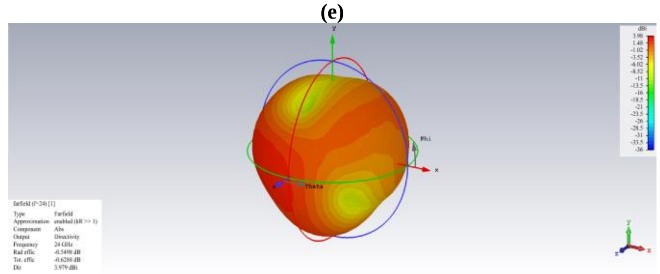

(f)

Fig. 7 The simulated 3D far-field radiation patterns at, (a)9GHz, (b)12 GHz, (c)15GHz, (d)18GHz, (e)21GHz, and (f)24GHz.

Following the simulation, antenna postprocessing was conducted for SAR values at 9.1 GHz and 24.2 GHz. A Four-layer human tissue phantom comprising skin, fat, muscle, and cortical bone is utilized in this analysis. Dielectric material properties of these tissues at the test frequencies, as per the data available on the Italian National Research Council website, are depicted in Table 2 below [16].

Table 2. Four-layer human tissue phantom dielectric properties at test frequencies of 9.1 GHz and 24.2 GHz

Human Tissue	9.1 GHz		24.2 GHz	
	ε_r	σ (S/m)	ε_r	σ (S/m)
Dry Skin	32.155	7.004	18.859	23.005
Fat	4.672	0.520	3.828	1.500
Muscle	43.989	9.334	27.074	29.666
Cortical Bone	8.406	1.934	5.522	4.505

Results obtained after simulation and postprocessing are shown in Figure 8 below. For the separation of 10 mm from the layered human body Phantom model, the value of SAR is 0.438 W/Kg for 9.1 GHz and 0.482 W/kg for 24.2 GHz for 1 g tissue with 10 mW input power.

These values are well below the guidelines as per FCC regulations (1.6 W/Kg for 1 gm). The proposed antenna is also tested for SAR values for a separation of 7 mm, which also gives the values below the FCC regulations.

The proposed antenna thus satisfies the crucial requirement of SAR value as per FCC regulations and meets the requirement of a wearable antenna for UWB and mm Waves.

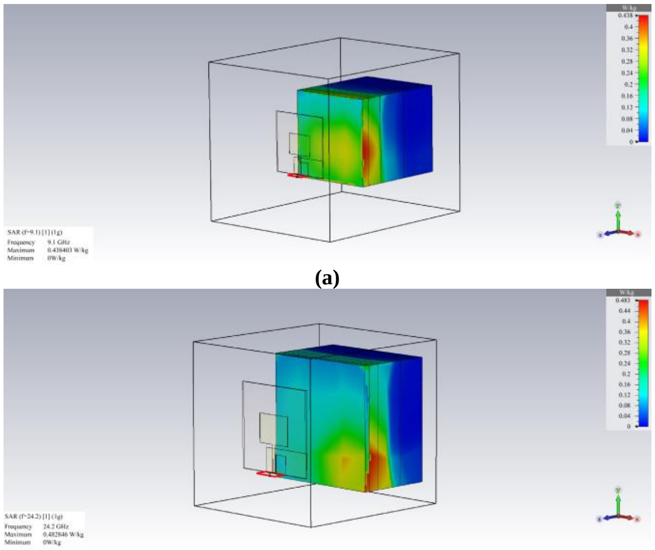

(a)

(b)

Fig. 8 Simulated SAR values of the proposed antenna: (a)9.1GHz, and (b)24.2GHz.

4.1. Measurement Results

A prototype of the proposed antenna is constructed using 0.254 mm thick Rogers RT/5880 semi-flexible laminate. Measurements are performed on Keysight PNA Vector Network Analyser (VNA) and anechoic chamber for Gain, Directivity, Radiation Pattern, and Return Loss measurements over the operational frequency band.

The realised Gain (dBi) versus frequency graph depicted in Figure 9(a) shows excellent agreement between the measured and simulated values, with the peak gain of 3.4 dBi at 21 GHz, with some minor deviations at 15,17, 24, and 30 GHz. The gain of the proposed antenna, which ranges from 2 to 3.4 dBi throughout the operational frequency span, is well-suited for Body Centric Communication Systems. Such moderate gain values maintain the excellent trade-off between sufficient signal strength and low SAR levels while maintaining compactness, which are crucial for wearable devices operating over short ranges for on-body and off-body communication systems.

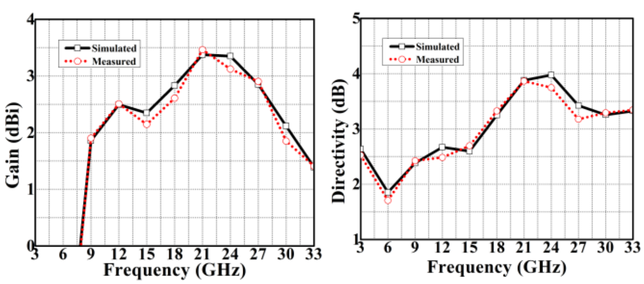

(a) (b)

Fig. 9 Plots of, (a)Gain, and (b)Directivity of the fabricated Prototype.

The plot of directivity for simulated and measured values is shown in Figure 9(b), which also shows an excellent match with some deviations at the higher frequencies of 21 and 27 GHz. The peak measured value of 3.74 dB at 24 GHz shows a difference of 0.23 dB from the simulated value. It is typical as well as effective for low-profile wearable antennas used for body-centric communication systems in the UWB and mm Wave bands, where high directivity is generally not preferred.

Radiation efficiency is an important parameter that quantifies how well an antenna transforms input radio frequency power to electromagnetic radiation, making it a crucial factor for assessing the performance of the antenna design.

Figure 10(a) below shows a plot of radiation efficiency for the designed prototype, which shows good agreement between simulated and measured values with some deviations. Radiation efficiency for the designed prototype shows the measured value varies from 60 % to 71.78 % over the operating frequency range, with a peak value of 97.56 % at 12 GHz.

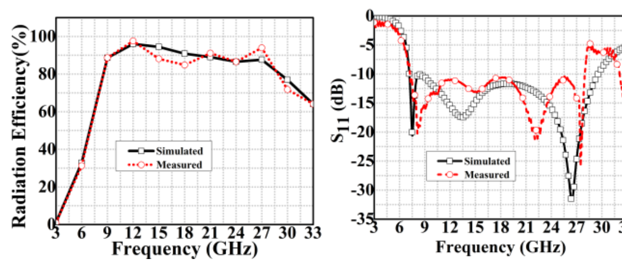

(a) (b)

Fig. 10 Plots of, (a)Radiation Efficiency, and (b)S_{11} for the proposed Antenna.

The S_{11} parameter simulated and measurement versus frequency plot is shown in Figure 10(b). This plot shows some differences in the nature of simulated and measured result plots, which are typical in the case of high-frequency broadband antennas. Such deviations normally occur due to manufacturing tolerances, heating effects at the time of soldering of the connectors, impedance variations happening due to the connector cables at the time of measurements, and reflection interferences due to open environment testing. The value of S_{11} remains below -10 dB threshold in the frequency span from 7.32 GHz to 27.96 GHz, showing the measured bandwidth of 20.64 GHz.

Figure 11 shows the Measurement setup with the proposed antenna prototype mounted for measurements in an anachoic chamber. The radiation pattern for the proposed antenna prototype is measured at 9 Ghz for the UWB band and 24 GHz for the mm wave band, and these measurements are compared with simulation results, which are depicted in Figures 12 and 13, respectively. Measured radiation patterns for Phi=0, Phi=90, and Theta=90 degree shows excellent agreement with simulated results, with some deviations.

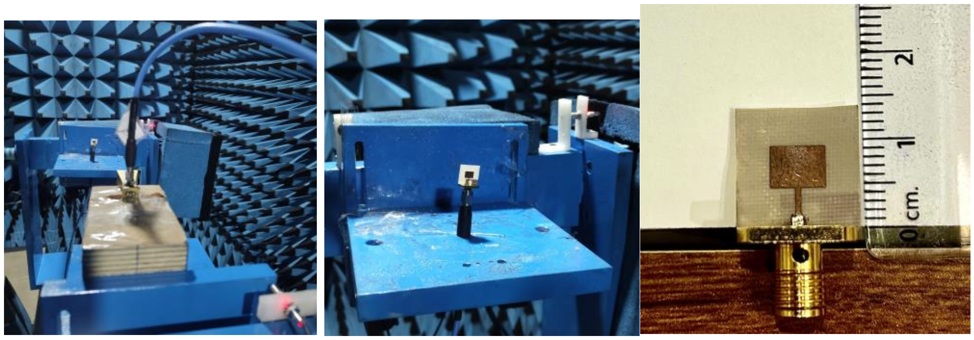

Fig. 11 Measurement setup with proposed antenna prototype mounted for measurements in an anachoic chamber

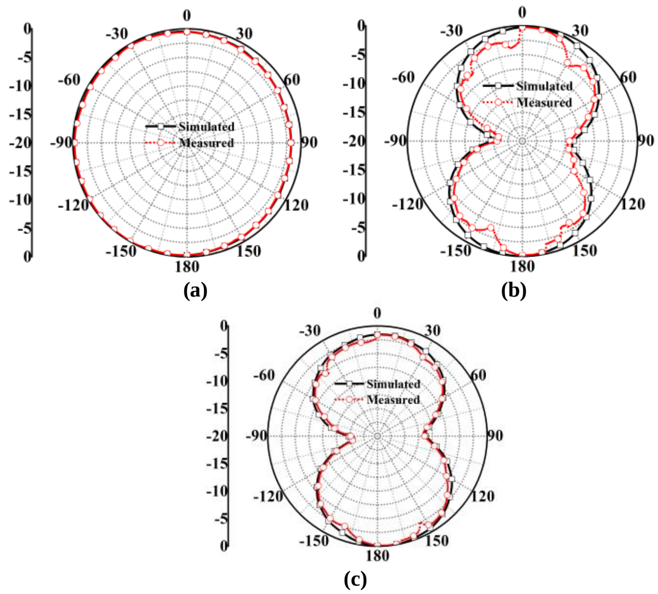

Fig. 12 Radiation pattern of fabricated prototype at 9 GHz for UWB range (a) Phi=0º (b) Phi=90º (c) Theta=90º

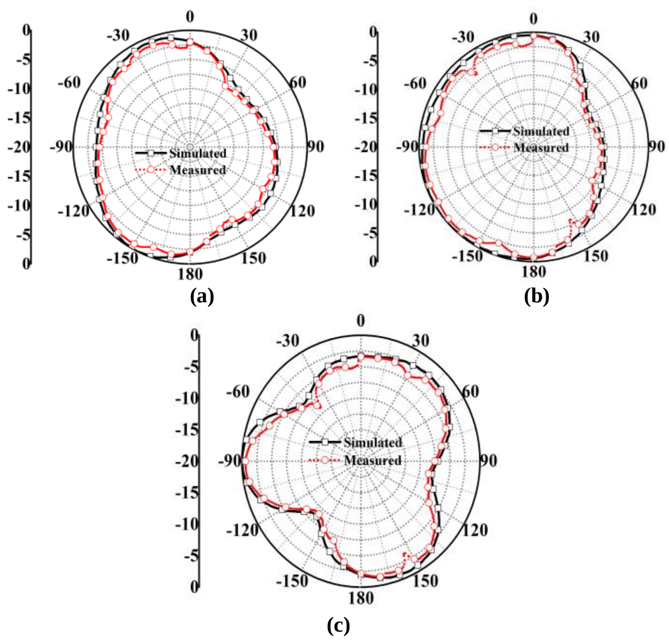

Fig. 13 Radiation pattern of fabricated prototype at 24 GHz mm Wave range (a) Phi=0º (b) Phi=90º (c) Theta=90º

The comparison between proposed work and state-of-the-art designs reported in recent studies [9-17] is shown in Table 3 below. The proposed work shows significant performance improvements over previously reported work owing to the adoption of systematic stepwise parametric analysis, where the influence of various parameters like patch dimensions, feed position, and ground plane geometry was systematically investigated to achieve optimal impedance matching, wider bandwidth, and desired gain for wearable applications. Each of these parameters was iteratively tuned through full-wave electromagnetic simulations until the desired performance characteristics were obtained, which was later validated with experimental results.

Because of this judicious material choice, structured design, and systematic optimization approach, the proposed antenna accomplished a wider measured bandwidth of 20.64 GHz, effectively covering both UWB and mmWave bands.

The low SAR values of 0.438 W/kg in the UWB range and 0.482 W/kg in the mmWave range further confirm the suitability of the proposed design for safe and reliable wearable applications. These results indicate that the proposed work is offering a distinctive advancement in wearable UWB/mmWave antenna design for next-generation body-centric wireless communication systems.

Table 3. Comparison of the proposed Antenna with previously published work

Ref. No.	Antenna Size (mm^3)	Operating Frequency (GHz)	Bandwidth (GHz)	Substrate	Method
9	30×20×0.8	3.1-23	19.9	FR-4	Partial Ground with DGS
10	200×220×1.57	0.5-23.5	23	TLY-5	Partial Ground with DGS
11	30×30×0.254	5.2-5.7 5.5 13.9	Tri-band	Rogers RT/5880	Partial Ground with DGS (MIMO)
12	20×20×1	4.3-30	25.7	Polyester	Monopole Fractal
13	60×40×1.52 Patch Thickness 28.5mm	1.39-160 (Simulated) 67 (Measured)	160 67	Rogers RO 3003	Partial Ground with DGS
14	25×40×1.5	2.2/5.7/7.7/8.3	1.4/1.1/0.3/0.1	Rogers RT/5880	Partial Ground with DGS
15	35×40×1	3.1-10.6	6.4	Felt Fabric	Partial Ground with DGS
16	16.19×16.19×0.254	24-24.5	0.5	Rogers RT/5880	Bow Tie with EBG Reflector
17	40×21	3-30	27	Not Reported	Fractal two-arm balanced
Proposed Work	**14.05×13.85×0.254**	**7.15-29.53 (Simulated) 7.32-27.96 (Measured)**	**22.41 (Simulated) 20.64 (Measured)**	**Rogers RT/5880**	**Partial Ground with DGS**

5. Conclusion

A Simple, Compact, Thin, Semi-Flexible, and Wearable UWB-mm Wave Microstrip Antenna with rectangular geometry and Partial ground having an integrated slot has been designed, and a prototype has been fabricated. The proposed antenna covers both the ultra-wide band and the 24 GHz mmWave band with an overall measured bandwidth of 20.64 GHz for various applications, making it a versatile antenna with low design complexity. The proposed antenna is developed using Rogers RT 5880 substrate with a substrate height of 0.254 mm, making it very thin. These features, along with its semiflexible property, enhance its suitability for various wearable applications in WBAN and medical wearables. These can benefit greatly from the high radiation efficiency of the proposed antenna, which allows for real-time transmission and monitoring of physiological parameters like body temperature, respiration, and ECG. It can be used for applications such as AR/VR wearable systems and smart textiles, which require ultra-fast, low-latency wireless links, which are provided by 24–30 GHz, which corresponds to the 5G mmWave band. Because of its small size and thin profile, it can also be used in wearable radar systems for motion tracking, fall detection, and gesture recognition. Additionally, these frequencies have potential for use in military and security applications, allowing for the integration of safe, short-range communications into tactical vests or smart helmets. Thus, the proposed ultra-wideband mmWave antenna, having a wide operational bandwidth, is ideal for next-generation wearable and body-centric wireless systems, as it offers a balance of bandwidth, antenna compactness, and integration potential. Further research will focus on wearability improvement with different substrates, along with an array of MIMO configurations for further throughput enhancements.

References

[1] Usman Ali et al., "Design, Analysis and Applications of Wearable Antennas: A Review," *IEEE Access*, vol. 11, pp. 14458-14486, 2023. [CrossRef] [Google Scholar] [Publisher Link]

[2] Shiban Kishen Koul, and Richa Bharadwaj, *Wearable Technology for Human Activity Monitoring and Recognition*, Wearable Antennas and Body Centric Communication: Present and Future, pp. 191-218, 2021. [CrossRef] [Google Scholar] [Publisher Link]

[3] Shahid Muhammad Ali et al., "Wearable and Flexible Sensor Devices: Recent Advances in Designs, Fabrication Methods, and Applications," *Sensors*, vol. 25, no. 5, pp. 1-43, 2025. [CrossRef] [Google Scholar] [Publisher Link]

[4] Sunaina Singh et al., "A Comprehensive Review and Analysis of the Design Aspects, Structure, and Applications of Flexible Wearable Antennas," *Telecom*, vol. 6, no. 1, pp. 1-31, 2025. [CrossRef] [Google Scholar] [Publisher Link]

[5] Dinesh Venkatachalam et al., "Compact Flexible Planar Antennas for Biomedical Applications: Insight into Materials and Systems Design," *Bioengineering*, vol. 10, no. 10, pp. 1-32, 2023. [CrossRef] [Google Scholar] [Publisher Link]

[6] Vivek Kumar, and Bharat Gupta, "Design Aspects of Body-Worn UWB Antenna for Body-Centric Communication: A Review," *Wireless Personal Communications*, vol. 97, pp. 5865-5895, 2017. [CrossRef] [Google Scholar] [Publisher Link]

[7] Faisal Mehmood, and Asif Mehmood, "Recent Advancements in Millimeter-Wave Antennas and Arrays: From Compact Wearable Designs to Beam-Steering Technologies," *Electronics*, vol. 14, no. 13, pp. 1-26, 2025. [CrossRef] [Google Scholar] [Publisher Link]

[8] Vikash Kumar Jhunjhunwala et al., "Flexible UWB and MIMO Antennas for Wireless Body Area Network: A Review," *Sensors*, vol. 22, no. 23, pp. 1-35, 2022. [CrossRef] [Google Scholar] [Publisher Link]

[9] MD. Firoz Ahmed et al., "An Ultra-Wideband Patch Antenna for Future Internet of Things Applications," *Journal of Science and Arts*, vol. 23, no. 4, pp. 1067-1080, 2023. [CrossRef] [Google Scholar] [Publisher Link]

[10] Fitri Yuli Zulkifli et al., "Super-Wideband Monopole Printed Antenna with Half-Elliptical-Shaped Patch," *Telecom*, vol. 5, no. 3, pp. 760-773, 2024. [CrossRef] [Google Scholar] [Publisher Link]

[11] Ayyaz Ali et al., "Design Process of a Compact Tri-Band MIMO Antenna with Wideband Characteristics for Sub-6 GHz, Ku-Band, and Millimeter-Wave Applications," *Ain Shams Engineering Journal*, vol. 15, no. 3, pp. 1-13, 2024. [CrossRef] [Google Scholar] [Publisher Link]

[12] Sumeet Singh Bhatia, and Jagtar Singh Sivia, "A Novel Design of Wearable Fractal Antenna for Wideband Applications," *2016 International Conference on Advances in Human Machine Interaction (HMI)*, Kodigehalli, India, pp. 1-4, 2016. [CrossRef] [Google Scholar] [Publisher Link]

[13] Shuvashis Dey, and Nemai Chandra Karmakar, "Design of Novel Super Wide Band Antenna Close to the Fundamental Dimension Limit Theory," *Scientific Reports*, vol. 10, pp. 1-15, 2020. [CrossRef] [Google Scholar] [Publisher Link]

[14] Waqas Ali et al., "Design and Analysis of a Quad-Band Antenna for IoT and Wearable RFID Applications," *Electronics*, vol. 13, no. 4, pp. 1-16, 2024. [CrossRef] [Google Scholar] [Publisher Link]

[15] Wanwisa Thaiwirot et al., "A Compact and Low Profile UWB All-Textile Antenna for WBAN Applications," *2024 Research, Invention, and Innovation Congress: Innovative Electricals and Electronics (RI2C)*, Bangkok, Thailand, pp. 128-131, 2024. [CrossRef] [Google Scholar] [Publisher Link]

[16] Mubasher Ali et al., "Ultra-thin EBG Backed Flexible Antenna for 24 GHz ISM Band WBAN," *2022 Antenna Measurement Techniques Association Symposium (AMTA)*, Denver, CO, USA, pp. 1-4, 2022. [CrossRef] [Google Scholar] [Publisher Link]

[17] Mohamed Salah Fouad et al., "Super-Wideband Fractal Antenna for Future Generations of Wireless Communication," *Progress In Electromagnetics Research C*, vol. 136, pp. 137-149, 2023. [CrossRef] [Google Scholar] [Publisher Link]